PHOTOCONDUCTIVITY IN STANNIC OXIDE CRYSTALS

By

JAMES EDWARD HURT

Bachelor of Science

Oklahoma State University

1957

Submitted to the Faculty of the Graduate School of
the Oklahoma State University
in partial fulfillment of the requirements
for the degree of
MASTER OF SCIENCE
May, 1959

PHOTOCONDUCTIVITY IN STANNIC

OXIDE CRYSTALS

Thesis Approved:

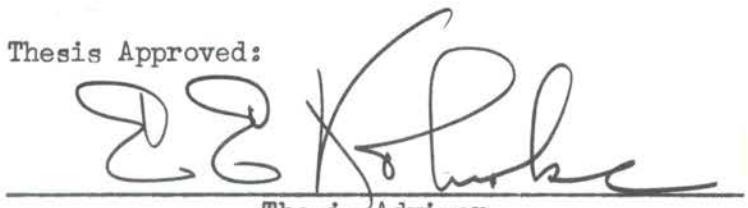

Thesis Adviser

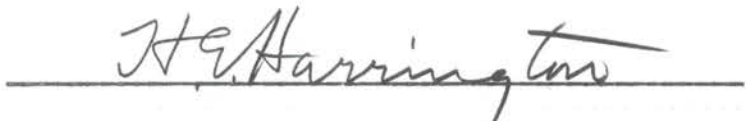

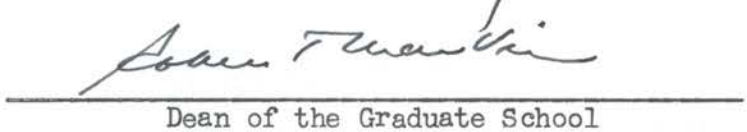

Dean of the Graduate School

This research was supported by the
Office of Naval Research under
Contract No. NONR-2595(01)

ACKNOWLEDGMENT

The author wishes to express his deepest gratitude to Dr. E. E. Kohnke for his valuable guidance throughout the course of the work, to the Office of Naval Research for sponsoring this research, and to the Oklahoma State University Research Foundation for their support. He is also greatly indebted to several members of the physics faculty for the loan of equipment and for helpful suggestions, to A. J. Belski and H. L. Hardway for their cooperation in experimental work, and to H. Hall, F. Hargrove, and R. C. Robertson for their preparation of samples and construction of special apparatus.

TABLE OF CONTENTS

LIST OF TABLES

LIST OF FIGURES

CHAPTER I

INTRODUCTION

With the increased interest in semiconducting materials during the last decade, the investigation of the solid state properties of some relatively commonplace substances, including several metallic oxides, has been pursued with growing enthusiasm. The simple oxides having electrical properties that cannot be classified as either purely electronic or purely ionic, form a group of semiconductors that is highly interesting. Being of a basic structure similar to that of other binary compounds, including semiconducting sulfides, selenides, tellurides, and halides, oxides may be expected to possess properties which can be correlated with those of such compounds. Photoconductive behavior is only one of a number of such properties, but it is of special interest because of the information it can furnish with regard to energy band structure and the conduction mechanism.

Oxides in general have high melting points, show pronounced chemical stability at low temperatures, occur naturally in either crystalline or amorphous forms, and have a basic energy band structure which is characteristic of the semiconductor category. They may be studied as powders, sintered agglomerates, thin crystalline films, or single crystals. However, as a rule all samples of a given oxide will not exhibit identical properties, owing to differences in impurity content or methods of preparation.

Several oxides have been subjected to extensive physical studies, these being principally oxides of copper and zinc and the magnetic oxide of iron. Within the last few years, some studies have been made of the properties of rutile, one of the three crystalline forms of the tetravalent oxide of titanium. (1, 2, 3). Thus far, information on the group of oxides as a whole is scattered, and no general conduction mechanism has gained acceptance. The present work has been undertaken in order to gain a better understanding of the electrical properties of the rutile family of oxides by investigation of the photoconductivity in stannic oxide, a close relative of rutile, and should supplement that of Northrip (4) on the optical absorption and electrical conductivity of stannic oxide.

Cassiterite is the form in which stannic oxide occurs naturally and is the form chosen for this study. It is the most common tin-bearing mineral, and hence finds commercial importance as the chief ore of tin. Extensive deposits are mined in Australia, Bolivia, Indonesia, Japan, and South Africa, and lesser deposits are to be found scattered over much of the land area of the earth. In past centuries a great part of the world's tin supply came from mines near Cornwall, England. Cassiterite is usually found in veins of igneous rock formed at high temperatures, such as granite or quartz, and is often found in alluvial deposits formed in regions where such veins exist. This mineral occurs in numerous localities in the United States, but no large deposits are known. (5).

The crystal structure of cassiterite is ditetragonal bipyramidal, with each tin atom surrounded by six oxygen atoms very nearly forming a regular body-centered octahedron. Each octahedron shares two

opposite edges with neighboring octahedra, and each of the two remaining points is shared with two octahedra having a common edge containing this atom. Every atom that takes part in edge-sharing forms one of the non-edge-sharing points of a third octahedron. Thus each oxygen atom vertex is shared by three octahedra, and the ratio of oxygen atoms to tin atoms is as indicated in the chemical formula SnO_2. Cassiterite crystals usually occur with considerable twinning, giving irregular crystal masses. Cleavage is not distinct, and best parting appears along the 111 or 011 planes. (5).

Cassiterite ranges in color from clear through yellow and red to opaque brown or black. An individual crystal may show an appearance varying from uniform coloration to a disorderly array of patches differing widely in color and transparency. The amount and nature of coloration are dependent on impurities and on deviations from stoichiometry. Cassiterite has a specific gravity near seven and a hardness between six and seven. The melting point is above 1100°C., but decomposition also occurs in the same temperature range. Chemically, stannic oxide reacts readily only with strongly alkaline compounds, forming stannic hydroxide in such reactions. It is insoluble in water, acids, and organic solvents. (6).

An interesting optical property of cassiterite is its birefringence, which shows an increase with increasing wavelength or increasing temperature. Both indices of refraction are near two, and tend to decrease with increasing temperature. Dichroism has also been observed in cassiterite, with the absorption of the extraordinary ray greater than that of the ordinary ray. (5).

The uses of this cyrstalline form of stannic oxide, other than its principal use as the chief source of tin metal, are numerous and varied. It finds application as an agent for producing opacity in glass, and as a base for colored glazes, particularly red and yellow ones. (7). Its resistance to corrosion and to thermal shock has in recent years made it useful as a component of refractory materials. (8). A ceramic material made from a mixture of powdered cassiterite and rutile has a very low temperature coefficient of capacitance. (7). Also in the powdered form, cassiterite is useful in industrial chemistry as a catalyst in the manufacture of hydrogen and carbon monoxide from hydrocarbons, the oxidation of hydrocarbons, and the hydrogenation of benzene compounds. (9). Thin electrically conducting coatings of stannic oxide on glass find application in de-icing equipment. (10). Treatment of cassiterite granules with hydrogen produces pressure dependent electrical resistance granules suitable for use in a device such as a microphone. (11). Addition of titanium ions to cassiterite produces a material that shows a green luminescence when irradiated with ultraviolet light or an electron beam. (12). Some industrial electrical contacts are made of a mixture of silver with from two to fourteen percent stannic oxide. (13). In transistor research, cassiterite has been tested as a filamentary transistor and found to show transistor action with a gain of 3.3. (14).

The purpose of the project of which this study is one phase is basic reasearch, the principal objective being the construction of an energy level diagram for a stannic oxide semiconductor, but it is quite possible that the information gained will suggest new practical applications for this semiconducting oxide.

CHAPTER II

PROPERTIES OF SEMICONDUCTING OXIDES

The literature on the properties of oxide semiconductors is relatively extensive, and it would be impractical to give a complete survey of the field here. As review articles, three that are quite useful and representative of the field are those by Verwey (15), who discusses electrical properties from a standpoint of dilution, stoichiometry, and controlled valency, and Gray (16, 17), who considers mainly surface effects.

A more comprehensive survey has been made of the published works on tin and titanium oxides in particular, the latter, of course, being the prototype rutile-structure material. Optically, both are birefringent and have refractive indices in the neighborhood of two or greater. (18, 19, 20). Rutile (TiO_2) shows one of the greatest known degrees of birefringence. Its ultraviolet absorption edge is near 4100 Angstrom units (A) (1, 2), corresponding to an energy gap of slightly over three electron volts (ev), while that of stannic oxide, as measured for thin films, is near 3000 A, giving an energy gap width of 4.1 ev. (21, 22). On the other hand, reported room temperature short wavelength absorption edges for natural cassiterite (SnO_2) include 3320 A (23) and 3750 A. (24).

The most remarkable electrical property of rutile is its very high dielectric constant, with reported average values ranging up to

110 (25) and 114. (26). Connell and Seale (27) found an anomalous dispersion of the dielectric constant in the frequency range between 0 and 50 kc, but it has been reported by Berberich and Bell (26) that the value remains nearly constant at 114 in the radio frequency region and falls off rapidly to 7.42 at infrared frequencies. They also reported that cassiterite has a dielectric constant of 24 at low frequencies, which decreases to 4.11 at optical frequencies. They further found, in agreement with the work of Schusterius (28), that the dielectric constant of rutile decreases with increasing temperature.

Extensive studies of the electrical properties of rutile were carried out by Cronemeyer and Gilleo (1, 2), who were concerned with ceramic samples and artificial single crystals. They measured optical absorption, photoconductivity, conductivity as a function of temperature, and Hall effect, and correlated the data with calculated activation energies based on a simple atomic model. Values obtained were 0.74 ev for the activiation energy and 3.05 ev for the intrinsic energy gap. Carrier density calculated from their data is approximately $10^{20}/cm^3$. Breckenridge and Hosler (3) used conductivity vs. temperature and Hall effect data to calculate carrier concentrations and mobilities. These were correlated with a model in which activation energies were calculated, using the assumptions of trivalent titanium ion sites and oxygen vacancies in the lattice as primary contributors to the behavior. Mobilities were described in terms of interactions of carriers with the nonisotropic lattice. Using Cronemeyer's earlier measurement as a basis, Breckenridge and Hosler predicted an intrinsic energy gap of 3.67 ev for rutile, explaining Cronemeyer's lower value as being due to excitation of electrons from neutral or singly ionized Ti^{+3}-oxygen vacancy centers to the conduction band.

The most thorough investigations of the electrical properties of stannic oxide have used samples in the form of thin films. (22, 29). That the structure of these films is the same as that of cassiterite has been verified by X-ray diffraction studies (30), but their stoichiometry is doubtful, as is evidenced by Aitchison's comparison of resistivities of the films and stannic oxide in the form of cassiterite. (29). Values given include 3.6×10^{8} ohm-cm. for cassiterite and numbers on the order of 10^{-2} ohm-cm. for the thin films. Aitchison attributes this low resistivity to an excess of tin in the films, which would explain the n-type conduction observed. Ishiguro and coworkers (22) also observed n-type conduction, and report an effective carrier mass near 0.2 electron masses. Hall mobilities obtained by the latter investigators fall in the range between 15 and 35 cm^2/volt-sec, and they give resistivities on the order of 10^{-2} ohm-cm. Aitchison found that addition of impurities containing pentavalent ions lowered the resistivity while addition of impurities containing trivalent ions had the opposite effect. These results, in their respective order, are similar to those obtained by reduction of the oxide to an oxygen-deficient structure and by adding an excess of oxygen to stoichiometric stannic oxide. The carrier concentration of a stannic oxide film was found by Ishiguro and coworkers to be in the 10^{19}-$10^{20}/cm^3$ range, approximately the same as that of rutile. Values for resistivity and Hall mobility in rutile are given by Cronemeyer (2) as 10^{2} ohm-cm and 0.1 to 10 cm^2/volt-sec, respectively, and he observed n-type conduction in rutile.

The most detailed study of electrical conductivity in stannic oxide powders is that of Foex. (31). He used cylinders made by

compressing stannic oxide at a pressure of 3000 kg/cm^2. He made measurements of the resistivity over the temperature range between 20°C and 1200°C, and obtained two activation energies, 0.38 ev in the room temperature region, and 1.77 ev in the high temperature region. He reported differences in resistivity caused by variations in sample preparation and the occurrence of resistivity changes produced by heating in various atmospheres. Samples heated and cooled in an oxygen atmosphere showed the highest resistivity.

Using sintered samples of stannic oxide, Le Blanc and Sachse (32) obtained a room temperature resistivity of 10^8 ohm-cm. Guillery (33), using both powders and sintered samples in low temperature measurements, found values ranging from 10^4 to 10^8 ohm-cm. Fischer (21), using films, obtained a value of about 0.03 ohm-cm. Bauer (34), also using films, measured activation energies of 0.02 ev near 100°K and 0.05 ev near room temperature, and by Hall measurements obtained an electron mobility of 0.9 to 6.6 cm^2/volt-sec and a Hall constant of -0.35 cm^3/amp-sec. This compares with Fischer's results of 6 cm^2/volt-sec for the mobility and -0.2 cm^3/amp-sec for the Hall constant. Fischer also reported a free electron concentration of 10^{20}/cm^3. Using samples cut from cassiterite, Northrip (4) measured resistivities ranging from near 2 x 10^{-3} ohm-cm to near 10^5 ohm-cm and activation energies between 0.04 and 1.12 ev for different samples in different temperature ranges. Optical measurements on these samples and one artificial sample, also by Northrip, gave an ultraviolet absorption edge generally in the 3550-3600 A region, but with some exceptions. This corresponds to an intrinsic energy gap of from 3.44 to 3.49 ev. The infrared cutoff was found to be near 7.5 μ, but anomalies appeared

here also, probably caused by impurities or oxygen vacancies contained in some of the samples. Some samples showed visible permanent color changes after heating to temperatures ranging up to 850°C.

Rutile crystals have been observed to show some consistent color changes under various influences. Zerfoss, Stokes, and Moore (35) reported that opaque crystals heated in an oxygen atmosphere at 1000°C took on a transparent bluish color, then became pale yellow, as oxidation progressed. Johnson (36) investigated the effects of doping rutile with anions of different valencies, and found that those having valencies greater than four markedly changed the resistivity. This was attributed to the production of large numbers of Ti^{+3} ions within the crystal. Also, Johnson and Weyl (37) studied the effects of Ti^{+3} ions and oxygen vacancies on the electrical properties and color of rutile single crystals, and believe the color changes to be due to changes in the oxygen vacancy concentration.

Rutile single crystals of macroscopic size were first successfully sysnthesized in 1947 by the Verneuil method as reported by Alexander. (38). However, despite the similarities existing between rutile and cassiterite, no cassiterite crystals of greater than microscopic size have been produced under controlled conditions. This has made it necessary to use natural crystals, thin films, sintered samples, or powders in any physical study of stannic oxide. Of these forms, only natural crystals can approach the ideal form of the large single crystal, but such crystals have a distinct disadvantage in their lack of purity. Liebisch (39), in spectroscopic studies, has found that aluminum, calcium, iron, titanium, and tungsten constitute major impurities, and that many other elements may be present in lesser

amounts. Another experimental difficulty with cassiterite crystals is the small faults and fractures that are found in almost every sample.

A few macroscopic stannic oxide crystals having the cassiterite structure have been found in the firebrick linings of furnaces of tin smelters, mostly during the latter half of the nineteenth century. Arzruni (40) has reported on the finding of several such crystals in a smelter near Salzburg. They were found in corrosion pockets in a furnace lining, and had evidently grown over a period of years. Speculations were that they had been formed either by vapor condensation or by precipitation from a saturated solution, but no supporting evidence could be supplied for either contention.

Microscopic stannic oxide crystals have been artificially produced by several methods. Deville (41) passed dry hydrogen chloride gas over stannic oxide powder held in a tube at red heat, and along the walls of the cooler portion of the tube obtained a microcrystalline agglomerate showing the cassiterite structure. Levy and Bourgeois (42) precipitated microscopic platelets and needles from a stannic acid solution. The same polymorphism was reported by Wunder (43) to exist in crystals grown in a flame using a borax bead flux.

A comparison of the disadvantages inherent in the various possible physical forms of stannic oxide has been made, and for the project of which this study is one phase, natural crystals have been found to most nearly meet the requirements.

CHAPTER III

THEORY OF PHOTOCONDUCTIVITY IN SEMICONDUCTORS

The phenomenon of photoconductivity can be expected to occur in any solid substance in which there exists a forbidden energy gap between the valence band and the conduction band. Both semiconductors and insulators satisfy this requirement, but here only semiconductors will be considered. This material is a condensation of topics of interest in Shockley (44), Rose (45), and Wright. (46).

The expressions for the equilibrium densities of free charge in a semiconducting crystal (44) can be derived in general form by the use of Fermi-Dirac statistics and are found to be

$$n = N_c e^{-(E_c-E_F)/kT} = 2(2\pi m_e kT/h^2)^{3/2} e^{-(E_c-E_F)/kT}$$

for electrons, and

$$p = N_v e^{-(E_F-E_v)/kT} = 2(2\pi m_h kT/h^2)^{3/2} e^{-(E_F-E_v)/kT}$$

for holes, where N_c is the effective number of quantum states in the conduction band, N_v is the corresponding quantity in the valence band, E_F is the Fermi level, E_c is the energy of a carrier at the lower edge of the conduction band, E_v is the energy of a carrier at the upper edge of the valence band, m_e and m_h are effective masses of electrons and holes respectively, k is Boltzmann's constant, h is Planck's constant, and T is the absolute temperature.

Changes in carrier density can result from variations in quantities other than temperature. Among these are the increases produced by bombardment of the crystal with electrons or other charged particles, or with electromagnetic radiation of sufficiently high energy. Consider the case of a crystal on which light photons having energies in an arbitrary range are incident, and for which crystal the energy levels are as shown in Figure 1. There are three possible processes by which an electron or hole may become an active carrier. These are:

(1) A photon of energy $h\nu_1 = E_c - E_v = E_G$, where E_G is the width of the forbidden energy gap, is absorbed in the crystal, and the energy of the absorbed photon shows up as the energy which raises an electron from E_v to E_c. This process activates two carriers, since the removal of the electron from the valence band leaves a hole in the valence band.

(2) A photon of energy $h\nu_2 = E_1 - E_v$ is absorbed in the crystal with the absorbed energy serving to move an electron from E_v to the bound state at E_1. This electron cannot act as a carrier, but the hole left behind in the valence band is free to transport charge.

(3) A photon of energy $h\nu_3 = E_c - E_1$ is absorbed in the crystal, with the absorbed energy raising an electron from the bound state at E_1 to the conduction band. One carrier, the electron, is produced by such an absorption.

The cross sections for capture of a photon by an atom in the crystal lattice reach maxima at photon frequencies ν_1, ν_2, and ν_3, for processes (1), (2), and (3) respectively.

As soon as the first excess free carrier is produced by a photon absorption, there is a nonequilibrium condition set up in the crystal. In order to regain equilibrium, there will be a tendency toward

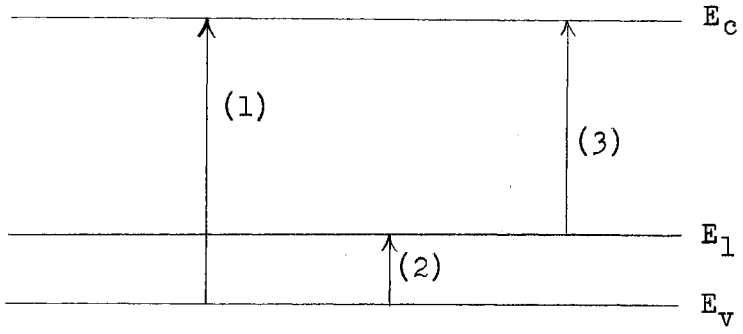

Figure 1.

Energy Levels Involved in
Photoconductive Processes.

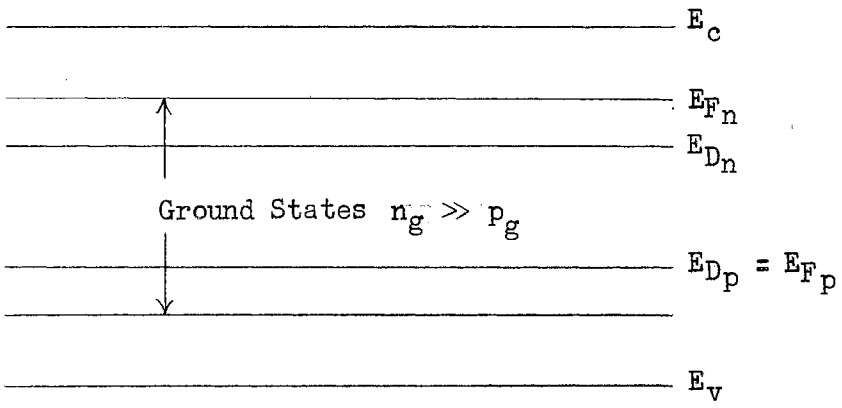

Figure 2.

Location of the Demarcation Levels
and the Steady State Fermi Levels.

elimination of excess carriers in the crystal, by processes which are reversals of (1), (2), and (3). If the crystal is left under a steady illumination for a sufficiently long time, the excess carrier densities will reach constant values, with the rate of generation, above the thermal rate of generation, becoming equal to the rate of recombination.

Consider the simplest possible example of a crystal in such a state, that of one having no recombination levels intermediate between E_V and E_c. In this case the only process acting to produce free carriers other than those produced thermally is the excitation of electrons from the valence band to the conduction band, with one free hole and one free electron resulting from each excitation. Thus, if Δn is the density of free electrons and Δp is the density of free holes produced by photon absorption, then $\Delta n = \Delta p$. Now assume these densities have become constant, the rates of generation and recombination being equal. Designate the number of excess carriers generated per unit time in a unit volume by g, and the average lifetime of a carrier by τ. In the case considered here, $g_h = g_e$ and $\tau_h = \tau_e$. The product $g\tau$ gives the number of excess carriers in a unit volume of the crystal in the steady state. Thus $g\tau = \Delta n = \Delta p$.

The generation rate g is a function of the number of photons entering a unit volume of the crystal per unit time and the cross section for the absorption of one such photon. This latter quantity in turn depends on the width of the energy gap E_G and the frequency ν of the incident photons.

The lifetime τ can be expressed as $\tau = (nsv)^{-1}$, where n is the free carrier density, v is the thermal velocity of free carrier, and s is the cross section for recombination of free carriers. A long

lifetime corresponds to a low transition probability. The usual orders of magnitude given for n, s, and v, are, respectively, $10^{11} \leqq n \leqq 10^{19}$ /cm^3, $10^{-22} \leqq s \leqq 10^{-12}$ cm^2, and $v \simeq 10^7$ cm/sec. This points to $10^{-12} \leqq \tau \leqq 10^4$ sec as a range of allowable values for the lifetime. τ is not independent of temperature, since this quantity has an effect on capture cross sections in the crystal. Also, for crystals having recombination states in the energy gap, the temperature influences the density of these states. In this latter case, τ is not to be confused with the decay time, which is the time required for the photocurrent to decay to a value 1/e times its maximum value.

Now consider this semiconducting crystal as an element of an electrical circuit, the crystal having two opposite faces separated by a distance L, each face attached to leads by ohmic contacts. With a potential difference V between these two electrodes, the electric field across the crystal is $E = V/L$. The transit time T_c for a carrier in the crystal is given by $T_c = L/E\mu = L^2/V\mu$, where μ denotes carrier mobility. For a carrier with a lifetime τ and a transit time T_c, the gain is defined as $G = \tau/T_c$. This number represents the number of charges that will be carried from one electrode to the other as a result of the absorption of one photon. Ohmic contacts are a necessary condition here, because for each carrier passing into one electrode, a similar carrier must enter the crystal at the opposite electrode to conserve total charge within the crystal.

The current flowing through such a crystal can be separated into two components, the "dark current" I, transported by thermally excited carriers, and the photocurrent I_p which is transported by the excess carriers resulting from absorption of photons in the crystal. For an

excess carrier density Δn, the corresponding charge density is $e\Delta n$, where e is the charge per carrier. Given that the transit time of this type of carrier is T_c, the photocurrent may be expressed as $I_p = e\Delta n/T_c = eg\tau/T_c$.

If the flow of photons into the crystal is terminated, the number of excess carriers diminishes until thermal equilibrium is regained. In the case discussed in the preceding paragraphs, rise and decay curves representing both excess carrier density and photocurrent approximate simple exponential functions of time, with a time constant equal to τ. When an electron in the conduction band falls into the valence band, the energy lost by the electron appears as the energy of a photon emitted from the crystal. The frequency of this radiation is the same as the frequency at which the fundamental optical absorption edge of the crystal is found. Emission of radiation of this frequency from the crystal is often termed "edge-emission".

This type photoconductor, while in the steady state (I_p constant), possesses what are known as "steady state Fermi levels", one for holes and one for electrons. These are defined by

$$n = N_c e^{-E_{Fn}/kT}$$

and

$$p = N_v e^{-E_{Fp}/kT} ,$$

where E_{F_n} is the difference between E_c and the steady state Fermi level for electrons and E_{F_p} is the difference between E_v and the steady state Fermi level for holes.

Photoconductors having bound states between E_v and E_c are not so simply described. These bound states may act as recombination

centers, deep trapping centers, or shallow trapping centers, and may be caused by impurities, dislocations, surface states, defects introduced by quenching or by bombardment with subatomic particles, or by any combination of these. The excitation processes occurring in a crystal may be of all three previously described general types, with variations of each of these. In the case of a photoconductor having one or more of these states in the energy gap, Δp is not necessarily equal to Δn, and τ_h is not necessarily equal to τ_e.

In a photoconductor, the demarcation levels are defined as the energy levels at which upward and downward transitions are equally probable. The demarcation levels for electrons and holes, which do not necessarily coincide, will be denoted here by E_{Dn} and E_{Dp}, respectively. The locations of the demarcation levels, along with those of the steady state Fermi levels, are shown in Figure 2. The ground state levels and steady state Fermi levels for both holes and electrons, are separated by an energy difference of $kT(\ln n_g/p_g)$, where n_g is the number of ground states occupied by electrons and p_g is the number of ground states occupied by holes.

In a semiconductor, most recombinations occur in the region between the two demarcation levels. States between E_{Dn} and E_c having an appreciable cross section for the capture of free electrons act as shallow traps for electrons. Likewise, there may be states between E_v and E_{Dp} that act as shallow traps for holes. The energy of a carrier near the lower edge of the conduction band or the upper edge of the valence band is nearly in thermal equilibrium with a free carrier, and such a carrier easily returns by thermal excitation to the band in which it can transport charge. It should be emphasized that carrier lifetimes

do not include time spent in traps. Deep traps are located between the two demarcation levels. Using s_n and s_p to denote capture cross sections for electrons and holes respectively, a trapping center with $s_n \gg s_p$ acts as an electron trap, while one with $s_p \gg s_n$ acts as a hole trap. A carrier caught in a deep trap is much less likely to regain its status as a free carrier than one caught in a shallow trap. Both types of traps, in addition to recombination centers, may be present in a single crystal.

For fixed densities of trapping centers and recombination centers, E_{D_n} and E_{D_p} for the steady state can be altered by a change of donor or acceptor concentration. For fixed concentrations of donors and acceptors, these levels can be altered by changes in temperature or illumination. Increased illumination will increase the difference between E_{Dn} and E_{Dp} which may increase the number of deep traps or recombination centers. An increase in the number of recombination centers increases the probability of recombination, shortens carrier lifetimes, and lessens steady-state photocurrent and decay time. An increase in the number of deep traps has effects opposite to these. For a photoconductor with no trapping or recombination centers, Δn and Δp vary as the square root of the light intensity, and for one recombination level the variation is linear. For more complex energy band structures, the relation is not so simple.

The usual photoconductor has a sensitivity, defined as the relative photocurrent per unit light intensity, that varies as a power of the intensity somewhere between 0.5 and 1.0, the exact power being dependent on the type and distribution of bound states in the energy gap. (45). If the bound states are all of one class or nearly so, and have a

uniform distribution with respect to energy, the power is near unity. If two or more classes of bound states are present, and one is a sensitizing class (for instance a set of deep traps for holes in an n-type photoconductor), then as more bound states of the sensitizing class come into play, the photoconductor becomes increasingly sensitive. Such an increase in sensitization can be observed in a few photoconductors as increasing light intensity widens the separation between the steady state Fermi levels, with the result that the sensitivity varies as a power greater than unity of the light intensity. This type of behavior is referred to as superlinearity.

In an n-type photoconductor, where hole traps dominate the behavior, electrons form the greater percentage of free carriers. For this type of photoconductor, a temperature increase lowers E_F, decreases $E_{Dn}-E_{Dp}$ and reduces the sensitivity, while an increase in donor concentration has opposite effects, increasing $E_{Dn}-E_{Dp}$.

It has been mentioned that for the simplest possible photoconductor, the rise and decay curves approach an exponential function of time with τ as the time constant. For a photoconductor with several recombination levels, the response may approach a sum of exponential curves, each with a different time constant. Shallow traps tend to lengthen response time beyond the response time related to τ.

The ultimate worth of a photoconductor is determined by the signal to noise ratio, where the signal is I_p and the noise is the root mean square fluctuation of the current about its average. Major sources of noise are contacts at electrodes and internal surfaces in the crystal.

CHAPTER IV

PREVIOUS INVESTIGATIONS OF PHOTOCONDUCTIVITY IN STANNIC OXIDE AND RELATED COMPOUNDS

Stannic Oxide

The number of investigations of photoconductive properties of stannic oxide (22, 47) is limited and some differences appear in the results. Andrievskii and Zhuravlev (47) obtained positive results on irradiation of a polycrystalline film with ultraviolet light. Photocurrents up to 215 times the dark current were observed, and decay times ranged from 20 to 3000 seconds on the samples examined. It was found that the decay curve could be represented as a sum of exponential functions of time, with several time constants involved. They also reported that decay times decreased with an increase in illumination and that the steady state photocurrent increased as the square root of the light intensity.

A less detailed investigation, also on a thin film, by Ishiguro and coworkers (22) confirmed the long decay times, but a photocurrent of only about 0.01 times the dark current was cited. Differences in methods of sample preparation and illumination were probably responsible for this large difference. Observations by these latter investigators indicated that the ultraviolet absorption edge corresponds to the width of the energy gap.

Neither of these investigations gave any detailed information regarding the dependence of photoconductivity on electric field intensity or on the wavelength of the incident light.

Titanium Dioxide

As previously mentioned, a compound closely related to stannic oxide in which photoconductivity has been studied is the rutile form of titanium dioxide. The wavelength dependence has been investigated by Cronemeyer and Gilleo (1, 2), who used AC methods on some artificial single crystals. Their results indicated a peak response near 4100 A, corresponding to the ultraviolet absorption edge, and a long wavelength tail extending to at least 1.2μ.

Kennedy and coworkers (48) have observed decay times on the order of ten to twenty hours in compressed samples of this material, and have shown that illumination with light of wavelength near 3650 A produces an irreversible uptake of atmospheric oxygen in the sample. In the same study, it was found that the sensitivity of titanium dioxide as a photoconductor is greater in vacuum than in an ordinary atmosphere, and that permanent changes in the conductivity can be caused by oxygen adsorption.

Zinc Oxide

An oxide of different basic structure that has been fairly extensively studied is zinc oxide. Of special interest in the photoconductive behavior of this substance is its dependence on the ambient atmosphere. Medved (49) has made simultaneous measurements of DC photocurrent and photodesorption in sintered samples, and his data indicates a definite relationship between the two.

Using both AC and DC methods, Collins and Thomas (50) have noted decay times ranging from seconds to minutes and have found that the onset of photoconductivity coincides with the ultraviolet absorption edge. The fastest decay times were found with an atmosphere of wet oxygen, and greater sensitivity was observed in oxygen-free atmospheres. The mechanism proposed to explain this behavior consists of electron-hole pair production by the incident light, with the holes rapidly combining with surface oxygen atoms to detach them from the crystal. This leaves a surface layer with an abundance of zinc ions and an increased number of free electrons.

Other Oxides and Binary Compounds

A recent study by Peria (51) emphasized the role of trapping centers caused by the presence of impurities in the photoconductivity of magnesium oxide, which has a greater energy gap than the other oxides discussed here. Mitchell (52) has suggested that electron scattering by impurity centers has much to do with the resistivity of oxide semiconductors in general.

Other binary compounds on which investigations of photoconductivity have been made include a number of sulfides, selenides, and tellurides. A few, such as cadmium sulfide and lead sulfide, have found wide practical application.

CHAPTER V

DESCRIPTION OF SAMPLES AND THEIR PREPARATION

Description of Samples

The samples used for experimental work in this study afford a wide variety of appearance and intrinsic properties even though many of them were obtained from the same locality in Bolivia. The following descriptions are given in order of receipt in form suitable for experimental work. The first few were used by Northrip (4) in his study of conductivity and optical absorption.

Samples I, II, III. Sample I, cut from the opaque protion of a Bolivian crystal containing both dark and clear bands, has the shape of a rectangular prism, and originally was an opaque reddish brown in color. In some high temperature studies, it has undergone a permanent color change, being now generally translucent, with a dark red coloration having moved into all but a central area which is faintly yellowish green. Throughout this study, it has not been subjected to any more heating, and has shown no further change in appearance. Internal surfaces are visible to the unaided eye.

Sample II was cut from a clear portion of the same crystal, and is of a rectangular cross section, but with irregular ends. No coloration is in evidence, but discontinuities in the structure can be seen on close examination. Because of its particularly high resistivity and

photoconductive response, this sample was the one studied in greatest detail.

Sample III was also cut from a clear portion of this crystal, and except for having a greater width and lesser thickness, is of the same general shape as sample II. A small smoky wisp of brown coloration can be seen near one side, but other than this it has the appearance of being the most nearly perfect cyrstal yet made available for this study.

Samples SI, SIA, SIB, SIC. Later two small crystals from Araca, Bolivia were obtained through the courtesy of the Smithsonian Institute (Smithsonian Inst. Cat. No. R-8034). Both of these were partly opaque, but had some clear bands. A relatively clear slab was cut from a side of one of these crystals, to form a sample having as one broad face a natural pyramidal face. This sample, although transparent, has a slight bluish tinge and shows various degrees of brownish coloration is some areas. It has been cut into three smaller pieces since the completion of Northrip's study, and these all appear to have essentially the same optical and electrical properties as the original slab. All three are irregular in shape, except for the two broad faces, which are nearly parallel. SIA is the clearest of the three, and SIC the darkest. Some defects can be seen in the structure of each of these samples, with SIA having the fewest.

Samples AI and AII. Two crystals of artificial cassiterite have been made available for this study through the kindness of Professor M. Weil of the University of Strasbourg, France. Both crystals were found a number of years ago in tin smelters near Salzburg. They are very much alike in appearance except for size. Both are transparent, show a violet tinge, contain large inclusions, and have the shape of short

bars with square cross sections and irregular ends. Neither has been cut or polished, being of convenient size for the work in which they are involved.

Samples IV, V, VI, VII, VIII. These five samples were cut from the clearest portions of a crystal found near Araca, Bolivia. All were cut in the shape of a flat rectangular slab, and all have numerous visible defects, the number and type varying from sample to sample. All show areas of brown coloration, with IV, VII, and VIII having nearly opaque regions at one end. Except for some minute spots, VI is free of brown areas. On the other hand, the appearance of V is dominated by two wide dark bands, which vary in color from reddish brown to a very dark opaque brown. The degree of transparency in the clear portions of these samples also varies, with that of VI slightly clouded and that of IV considerably more clouded. A small triangle of extreme clarity can be seen at one corner of sample V.

Samples IX, X, XI, XIIA, and XIIB. These samples also were cut from clear portions of a crystal from near Araca, Bolivia, and like those described in the preceding paragraph, were cut in the form of rectangular slabs. All show numerous defects, but brown regions are limited to almost insignificant specks in IX and XIIA. All are quite transparent, with XI, XIIA, and XIIB showing a definite yellow-green coloration throughout. X is unique among the samples used in this study in that two major structural discontinuities within the sample can be seen to contain a yellow foreign substance.

The following table lists dimensions of the individual samples, along with short wavelength cutoff values, determined by Northrip (4) for samples I, II, III, SI, and AI, with the remaining values coming

TABLE I

DIMENSIONS AND SHORT WAVELENGTH CUTOFFS OF THE SAMPLES

SAMPLE	LENGTH (mm)	WIDTH (mm)	THICKNESS (mm)	SHORT WAVE-LENGTH CUTOFF (A)
I	5.6	3.9	1.4	4300
II	6.2	2.2	1.5	3550
III	5.7	3.2	0.95	3550
SI	7.4	5.3	1.0	3600
SIA	5.0	4.7	1.0	3550
SIB	7.2	3.4	1.0	3550
SIC	6.0	4.4	1.0	3550
AI	7.0	3.5	3.2	3550
AII	5.6	2.6	2.6	----
IV	8.3	5.0	0.91	3550
V	5.7	4.8	1.0	3700
VI	5.7	4.7	1.0	3600
VII	7.7	6.0	0.9	3450
VIII	10.7	6.1	1.0	3550
IX	8.3	5.5	0.96	3450
X	8.1	5.1	1.0	3500
XI	7.9	4.7	1.0	3970
XIIA	5.0	4.7	1.13	3750
XIIB	5.2	3.3	1.16	3800

from preliminary optical work on the more recently received samples. Dimensions given for samples of irregular shape are maxima, and absorption edge cutoff values given are for clear areas of crystals. An absorption edge cutoff at 3550 A corresponds to an energy gap of 3.49 ev.

Sample Preparation

The samples used in this study, except for AI and AII, were cut by a diamond saw from natural crystals, and the broad faces of each sample, except for the few cases were a natural face could be allowed to remain (SIA, SIB, and SIC), were polished to a finish sufficiently fine to permit optical studies. A number of abrasive powders, ranging from a fine grade of emery to jeweler's rouge, were used to bring the surfaces to a smooth flat finish, and a very fine alundum powder was used for the final polishing. It was necessary to use considerable care to prevent pitting, to which these surfaces show a high susceptibility.

When not in use in an experiment, the samples were kept in individual plastic vials and protected by cotton. In most experiments it was necessary to attach crystals to mounts or to electrical leads by an adhesive electrically conducting substance. This necessitated cleaning the crystal at the end of each experiment. The usual procedure for this consisted of an acetone bath to dissolve organic material that might be present, followed by a gentle swabbing with filter paper moistened with acetone. The sample was then allowed to dry, after which it was given an alcohol bath to dissolve any film formed by the acetone. Occasionally a bath in nitric acid was necessary to dissolve inorganic foreign materials.

Electrical contacts used in most experiments were of Aquadag, a colloidal suspension of graphite. When dry, these contacts were usually covered with a quantity of silver paint (Dupont 4817) to add mechanical strength. In all handling of samples, especially when making contacts, it was necessary to exercise great care in order to avoid smearing any material on the sample which might form a conducting path on its surface.

CHAPTER VI

EXPERIMENTAL EQUIPMENT AND PROCEDURES

Sample Holders

As most measurements with which this study is concerned were made at room temperature and pressure, the sample holders used were of elementary construction. The principal factors taken into consideration in mounting a crystal were the exclusion of light other than that used as the exciting source and the placement of insulation so as to prevent short circuiting of the crystal. Best results were obtained in both DC and AC measurements by using as electrodes a pair of strips of clean sheet copper, mounted and sprung so that a slight pressure would hold a crystal in place while contact materials dried. Such an arrangement could be enclosed in a light-tight box for DC measurements, with light admitted when desired by a camera shutter fixed in a wall of the box.

A limited number of measurements were made using the apparatus shown in Figure 3. The sample was clamped to the lower end of the stainless steel coolant chamber, as was a copper-constantan thermocouple junction. A copper bottom on this chamber helped to bring the sample and thermocouple junction to a temperature near that of the coolant. This sample holder was equipped with a fitting that enabled it to be housed in a Dewar vessel for low pressure studies. The Dewar vessel used was of fused silica, which is transparent to light of wavelengths in the near ultraviolet region. The coolant used in this

apparatus was acetone cooled by dry ice, and light was admitted to the sample by removal of the opaque sleeve-like cover of the Dewar vessel.

Because stannic oxide is only very slightly sensitive to wavelengths other than those in the ultraviolet region, sample holders used in AC measurements could be even less elaborate than the DC sample holders, with a permanent opening toward the source used for excitation. Effects produced by laboratory lighting could be detected only in DC experiments involving the most sensitive samples with no shielding precautions taken. This could be attributed chiefly to the comparatively small amount of ultraviolet radiation from fluorescent lights. The low-temperature sample holder described above could be used for AC measurements as well as DC measurements.

DC Apparatus

The system shown in Figure 4 was used for most measurements of DC photoconductivity. Current in the crystal circuit was supplied by a 67.5 volt "B" battery, and could be varied by a voltage divider. In series with the crystal were a microammeter for determining the dark current and two 100 ohm wire wound precision resistors, which by a switching arrangement could be used to act as a resistance of either 50 ohms $\pm \frac{1}{2}\%$, 100 ohms $\pm$ 1%, or 200 ohms $\pm$ 1%. In most cases, resistances of this order of magnitude were negligible compared to the resistance of the crystal. The potential difference across the precision resistance, accurately measured, could be used for determining the current through the crystal. Connected across this resistance were a Leeds and Northrup Type K2 potentiometer for potential difference measurements accurate to 10^{-6} volts, an adjustable

bucking voltage circuit for cancelling the potential difference due to the dark current, and a DC amplifier, the output of which was fed to a recording milliammeter. Used as the DC amplifier was a General Electric model 8901490G2 self-balancing potentiometer and the recorder was a Texas Instruments "Recti-riter" with a rectilinear chart. Though primarily a voltage amplifier, the self-balancing potentiometer was used as a current amplifier here, the input resistance being known and the coil resistance of the recorder being of a value specified for use with this amplifier. Necessary calibrations were carried out by means of the K2 potentiometer. Two shunt resistances were supplied with the amplifier, enabling use of the instrument in two ranges of amplification differing by a factor of ten. Three different available values of precision resistance made the entire system capable of six different amplification factors.

DC Measurement Procedures

The most elementary method of measuring DC photoconductivity and the one used on several occasions involved a series hookup of battery, crystal, and microammeter. The dark current was allowed to reach a steady value, then light was admitted to the crystal and current readings taken at equal time intervals. From the information thus gained, a rise curve could be plotted. Decay curves were obtained in the same manner, except that the light was blocked from the crystal. This method was always used for initial measurements of newly received samples, in order to ascertain the order of magnitudes of the crystal resistance and the photocurrent.

Using the more extensive circuitry described in the preceding section, two methods could be used for obtaining photocurrent rise and decay curves. The first of these involved measurements of the potential difference across the precision resistance by use of the K2 potentiometer, with the times of each reading and of the opening and closing of the shutter being noted. For this method of measurement, probably the most precise of any used, neither amplifier, recorder, nor bucking voltage circuit was used.

The other method, which involved the entire system, consisted of first measuring the dark current with the microammeter, then using the K2 potentiometer to determine a bucking voltage adjustment to balance the potential difference resulting from the dark current flowing through the precision resistor. After this balance was attained, the K2 was replaced in the circuit by the amplifier and recorder, which were set to show zero input. The system was allowed to run until it was assured that the current in the crystal circuit was stable and any tendencies of the instruments to drift had been found, if they existed. With the system in a steady state, zero current was recorded. With light allowed to fall on the crystal, and a photocurrent produced, the photocurrent alone was recorded, barring changes caused by unforeseen disturbances. Use of the highest amplification available in the system enabled photocurrent as small as 10^{-8} amperes to be detected. The largest photocurrent that could be recorded with this system was 4×10^{-5} amperes. If it was necessary to work with photocurrents larger than this, the recorder itself was placed in the crystal circuit, in series with the crystal, and no amplification used. This enabled measurement of photocurrents up to one milliampere.

With knowledge of chart speed and the input necessary to cause a full scale deflection of the recorder, considerable information regarding the form of the rise and decay curves and decay times could be obtained.

Spectral Sensitivity Measurements

Two methods, both involving DC measurements, were used to determine the relative sensitivity as defined in Chapter III, as a function of the wavelength of the incident light. One, which was effective for almost every sample showing any appreciable photoconductivity, but which was restricted to limited regions of the spectrum, used a mercury arc light source and a monochromator to obtain fairly intense light at selected wavelengths. The photocurrent produced at each wavelength was recorded and the curves for a particular sample at the wavelength of each strong line of the mercury spectrum were compared. For these measurements, it was necessary to determine the relative intensities of light of all wavelengths used as it left the monochromator. For this calibration, a type FJ-76 photoelectric tube, with a peak sensitivity in the ultraviolet region, was used.

The second method, which afforded a means of measurement using a continuous spectrum, but which could be used with only the most sensitive samples, employed the tungsten light source and optics of a Beckman DK-1 spectrophotometer. The crystal, in a series circuit with a dry cell and a microammeter, was mounted in the sample compartment of the spectrophotometer; the sample compartment cover was placed over the crystal and leads and taped down so as to exclude from the crystal light other than that originating in the instrument. The monochromator

was set at the desired wavelength and the light source selector adjusted to admit light from the tungsten source to the crystal. The current rise for an exposure of one minute was recorded and the light taken off the crystal. After the photocurrent had decayed, this procedure was repeated at a different wavelength. Measurements of this type were usually made using intervals of 50 A, each measurement having a bandwidth of 57 A in the absorption edge region. A curve of intensity vs. wavelength was obtained for the light source used, and data corrected for variations in intensity.

AC Apparatus

To provide an AC light source of variable frequency in the neighborhood of 15 cycles/sec, a chopper was built using a DC motor such that the chopping frequency showed a linear variation with applied voltage between 10 and 20 cycles/sec.

Used in conjuction with this chopper was the low-frequency amplifier shown in Figure 5. The input signal was obtained from a resistor in series with the crystal, and having a value less than one percent the resistance of the crystal. In the amplifier, selectivity was obtained by a twin T feedback circuit, with a one megohm input resistance reducing the input signal to a small enough amplitude that the signal fed back was of comparable size to the input in the range of frequencies to be cut out. Reduction of the input resistance decreased selectivity, but increased overall amplification. With no input resistance, selectivity was almost entirely absent, but the amplification was near 70, about 12 times greater than with a one megohm input resistance. Because of the small signals involved, it was often necessary to eliminate the input resistance.

AC Measurement Procedures

After the dark current in the crystal circuit reached a steady value, the crystal was exposed to a light source chopped at 15 cycles/sec. The signal originating at the series resistor was fed into the amplifier described in the preceding section, and the amplified signal measured by means of an oscilloscope or an AC voltmeter. Before each use of the amplifier for these measurements, a 15 cps signal of known amplitude was fed into the amplifier and the resulting output measured to determine the amplification factor. With knowledge of this number, the direct current in the crystal circuit, and the resistance across which the signal was taken, the percentage increase of current produced by the incident chopped light could be computed. With i the direct current in the crystal circuit, R the resistance across which the signal was taken, A the amplification used, and V the amplified AC voltage, the fractional change in current was given by $\Delta i/i = V/ARi$. Since measurements involved only very small fractional current changes, the field across the crystal remained essentially constant, and $\Delta i/i$ could be considered as a close approximation to $\Delta\sigma/\sigma$, where σ is the conductivity of the crystal.

For many of these measurements, an AC voltmeter was used to read the rms voltage of the output signal, as magnitudes were more easily readable than on the trace of an oscilloscope. In order to convert rms values to base-to-peak values for the waveform involved, the output signal was measured simultaneously on voltmeter and oscilloscope at a number of different voltage levels, and the multiplicative factor obtained was 3.70 for the entire range of amplitudes.

The light source used in these measurements was the full spectrum of a mercury arc lamp, with a quartz lens placed between the lamp and the crystal to concentrate the light energy on the crystal.

In measurements of $\Delta i/i$ as a function of light intensity, a constant electric field was kept across the sample holder, and the intensity of the light incident on the crystal was varied by changing the geometrical arrangement of the light source, lens, and crystal. The intensity at the crystal produced by each arrangement used was measured by replacing the crystal with a Charles M. Reeder & Co. model RHL-7C vacuum thermopile. The intensities measured ranged from 45 to 314 microwatts per square centimeter.

To gain some indication of the importance of contacts in these measurements different sets of contacts were used, with the contact material being either graphite or indium.

To determine the dependence of $\Delta i/i$ on the applied voltage, values obtained for $\Delta i/i$ at a particular intensity in the set of $\Delta i/i$ vs. intensity determinations carried out at different voltages as described above were plotted as a function of voltage. This dependence was examined for several intensities, and was cross checked by investigating the response of the cyrstal with the light intensity held constant while the applied voltage was varied.

It was necessary to insure complete coverage of the crystal by the light source image, so that comparisons could readily be made among sets of data obtained at different light intensities.

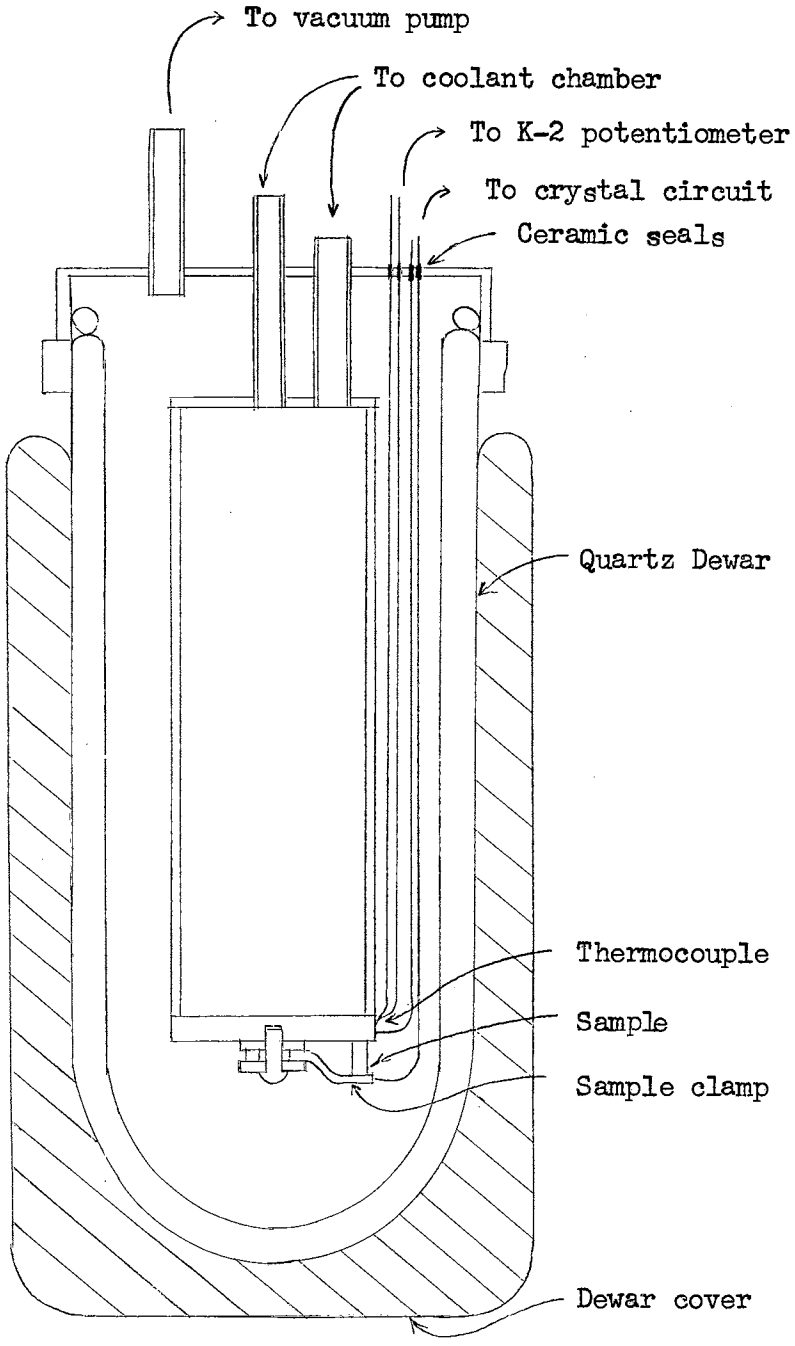

Figure 3.

Cross Section of Low-temperature Sample Holder.

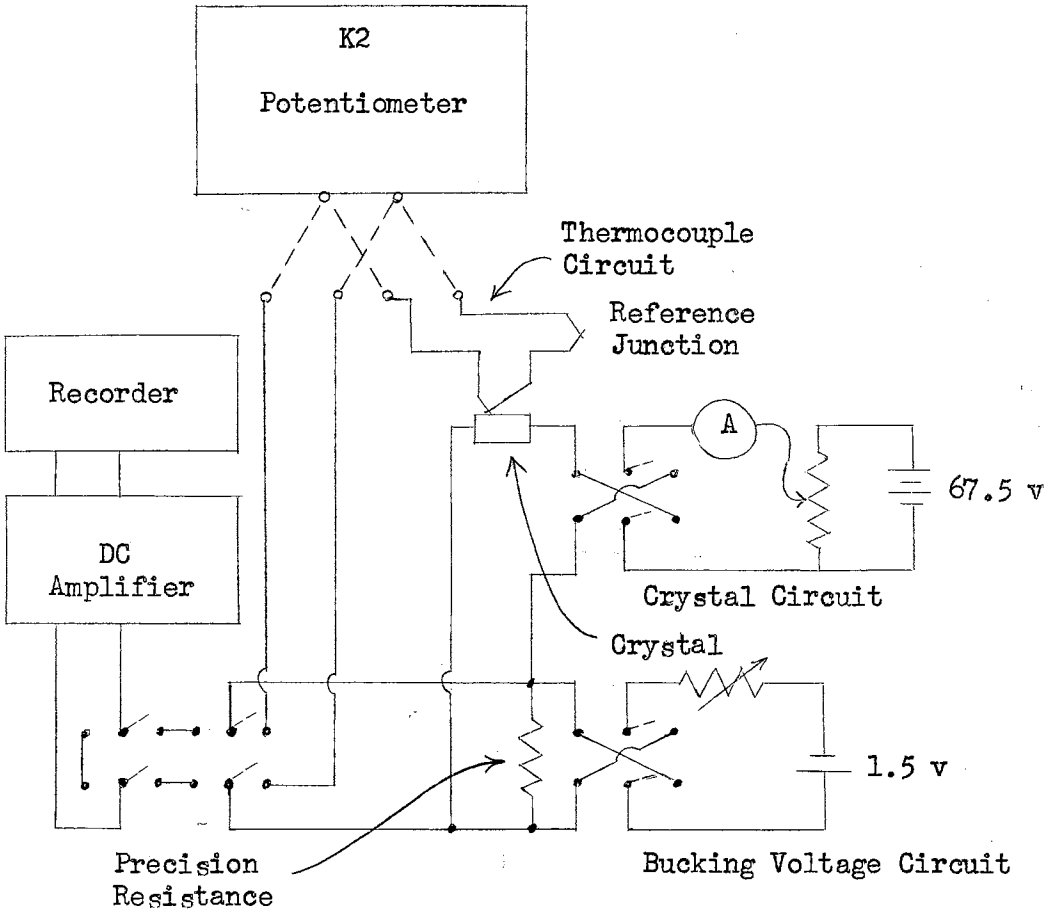

Figure 4.

Diagram of Circuitry Used in
DC Measurements.

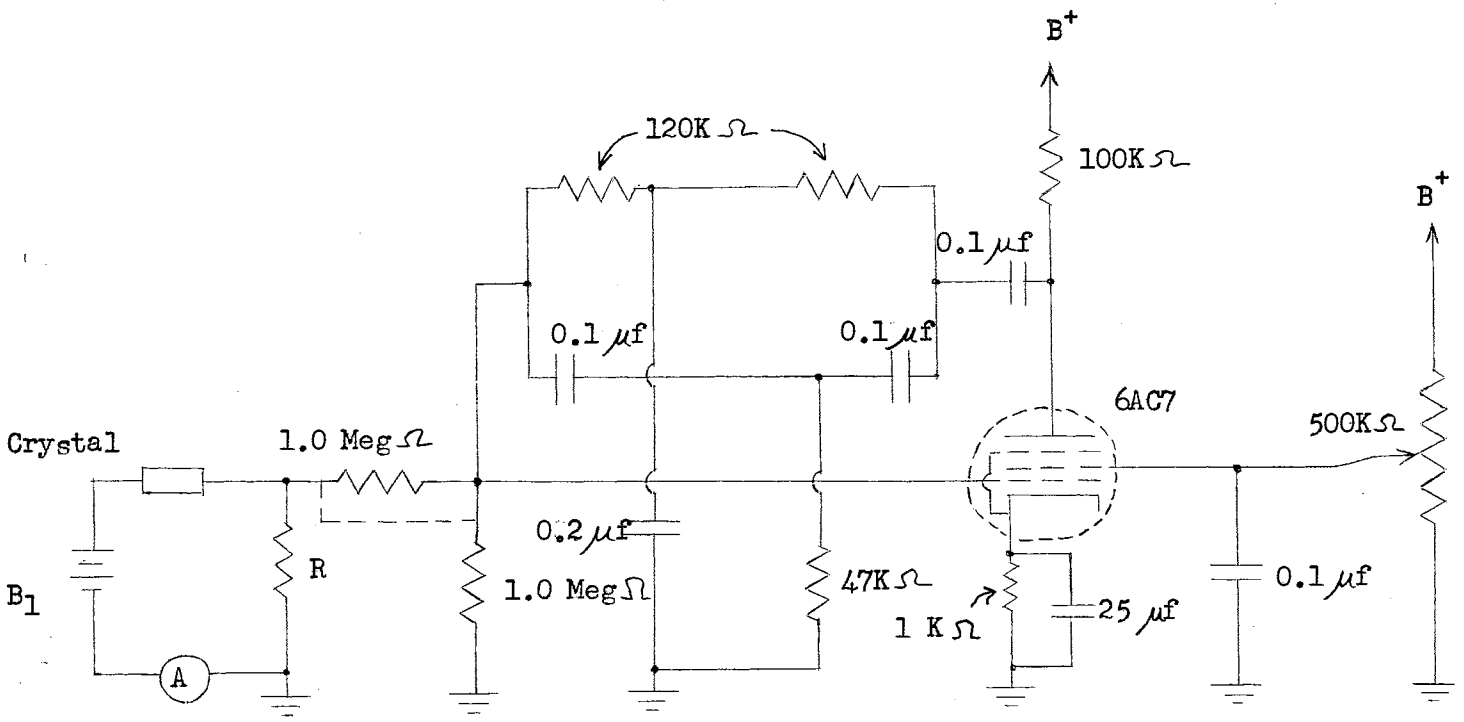

Figure 5.

Diagram of Circuity Used in AC Measurements.

CHAPTER VII

RESULTS

DC Photoconductivity

All samples available for this study were examined for photoconductivity by DC methods, using the full spectrum of a mercury arc lamp for illumination. Positive results were obtained for all samples except the Smithsonian smaple, the two artificial samples, and sample I. These samples were all of considerably lower resistivity than the other samples. The relative responses of all samples, based on percentage increase of current after a 15 second exposure to the light source, are listed in Table II. Values are based on the response of sample II, the one of greatest sensitivity.

TABLE II

RELATIVE DC PHOTORESPONSES

SAMPLE	RESPONSE	SAMPLE	RESPONSE
I	0.000	V	0.015
II	1.000	VI	0.017
III	0.014	VII	0.056
SIA	0.000	VIII	0.025
SIB	0.000	IX	0.008
SIC	0.000	X	0.010
AI	0.000	XI	0.012
AII	0.000	XIIA	0.040
IV	0.028	XIIB	0.012

Decay Time Variations

Some changes in the character of the rise and decay curves obtained in DC measurements were noted with increasing time of exposure. For an exposure of five minutes, for example, with sample II at room temperature, the decay time was under five seconds and the total current returned to the dark current level within twenty minutes. With an exposure lasting for a period of approximately three hours, on the other hand, the crystal also at room temperature, the decay time had increased to several hours, and residual photocurrent was still present after twenty to thirty hours in darkness. Rise curves, if recorded for periods exceeding twenty minutes, departed somewhat from the form expected by showing a slight increase of slope (dI_p/dt) with increasing time (t). This behavior was found to persist, and showed no indication of change even when the crystal was continuously illuminated for periods as long as 7.5 hours. Because of this behavior, no rise curve was recorded in which a steady state photocurrent was attained. Typical rise and decay curves for sample II are shown for a short exposure in Figure 6 and for a long exposure in Figure 7. Both curves were obtained using graphite contacts, room temperature, an applied voltage of 67.5 volts, and a full mercury arc spectrum.

Other trends were noted as a result of DC measurements at reduced temperatures and pressures. These indicated that both sensitivity and decay time decrease with decreasing pressure of the ambient atmosphere and with decreasing temperature.

Spectral Distribution

Response as a function of the wavelength of the incident light was investigated chiefly in samples II and III. The high sensitivity of sample II permitted reliable readings to be taken using the optics and tungsten light source of the Beckman DK-1 spectrophotometer. The results thus obtained are shown in the graph in Figure 8. Note that even with the low resolution previously indicated, a definite response peak is found which coincides with the measured ultraviolet absorption edge, and that a small amount of photoconductivity is detectable in the blue end of the visible spectrum.

Other measurements of the photoconductivity produced by monochromatic light were carried out with a mercury arc light source and a Gaertner monochromator. Rise and decay curves were obtained for samples II and III at wavelengths of 2537, 2967, 3131, 3650, 4047, and 4358 A. These tended to confirm response vs. wavelength data resulting from the measurements using the tungsten source, indicating that the one-minute response, corrected for intensity, at wavelengths both above and below 3650 A was less than that at 3650 A.

AC Photoconductivity

Response in samples II and III was investigated by AC methods as a function of the intensity of the incident light. The light used was the full spectrum of a mercury arc source, chopped at 15 cps, and focused on the crystal by a quartz lens. The signal produced was passed through a linear amplifier and observed by means of an oscilloscope or AC voltmeter. The response of sample II was measured with the range of applied

voltages extending from 20.1 to 129.0 volts, and that of sample III was measured over a range of voltages extending from 6.4 to 59.5 volts. Accurate values for the electric field strengths in the crystal cannot be given, since contact effects are not yet known in detail.

The composite results obtained for each crystal over the voltage ranges specified above are shown in the graph in Figure 9 at the end of this chapter. The abscissa represents the intensity of the light striking the crystal, with all values referred to a base intensity I_o, which at 44.9 $\mu w/cm^2$ was the lowest intensity for which data was obtained. The ordinate indicates the behavior of the response, with all values being referred to the value of $\Delta i/i$ obtained for the base intensity I_o. This quantity will here be denoted by $(\Delta i/i)_o$. The actual quantity represented by the ordinate then is $(\Delta i/i)/(\Delta i/i)_o$, the ratio of the fractional current increase at the intensity under consideration to that found for $I = I_o$. With the response plotted in terms of this quantity, and the applied voltage within the range of voltages for which the current through the crystal showed an essentially linear dependence on the applied voltage, it was found that all $(\Delta i/i)/(\Delta i/i)_o$ vs. intensity curves were identical within limits of experimental error. Thus for a given range of intensities, with applied voltages kept within the region of essentially constant resistance, an average curve characteristic of an individual sample could be plotted. The curves shown in Figure 9 are such average curves, one being computed from the results of 4 determinations with sample II, and the other that obtained from the results of 29 determinations with sample III.

Of the 29 curves obtained for sample III, 25 involved the use of graphite contacts and 4 involved the use of indium contacts. It was

interesting to note that there was no noticeable difference between the $(\Delta i/i)/(\Delta i/i)_o$ vs. I curves obtained with indium contacts and those obtained with graphite contacts. However, if magnitudes of $\Delta i/i$ are to be considered, differences were quite apparent, as evidenced by the fact that values of this quantity obtained for an intensity of 156.1 $\mu w/cm^2$ clustered near 0.0045 for indium contacts and near 0.0102 for graphite contacts. All data for sample II were obtained with graphite contacts, with values for $\Delta i/i$ at an intensity of 156.1 $\mu w/cm^2$ lying in the neighborhood of 0.0019. Applied voltages near 60 v were used here.

In connection with these light intensity dependence measurements, the dark current in both samples was measured as a function of the applied voltage. The curves for both samples indicated an essentially linear dependence of current on voltage at low voltages, and a decreasing resistance at higher voltages, with an eventual breakdown found for sample III, the sample of lower resistance. The fact that the resistance of sample II did not break down even at 300 volts implies that the point of breakdown is dependent on the carrier density rather than the electric field strength, the two samples being of similar dimensions. The curve for sample II is shown in Figure 10 and that for sample III is shown in Figure 11.

Observed decay times for short-period illuminations produced by the chopping of the light were less than 10^{-3} seconds, indicating a domination of the AC behavior by the faster states present in stannic oxide. However, "slow" states were not completely absent, since the direct current level showed a slight increase during the time the crystal was exposed to the chopped light.

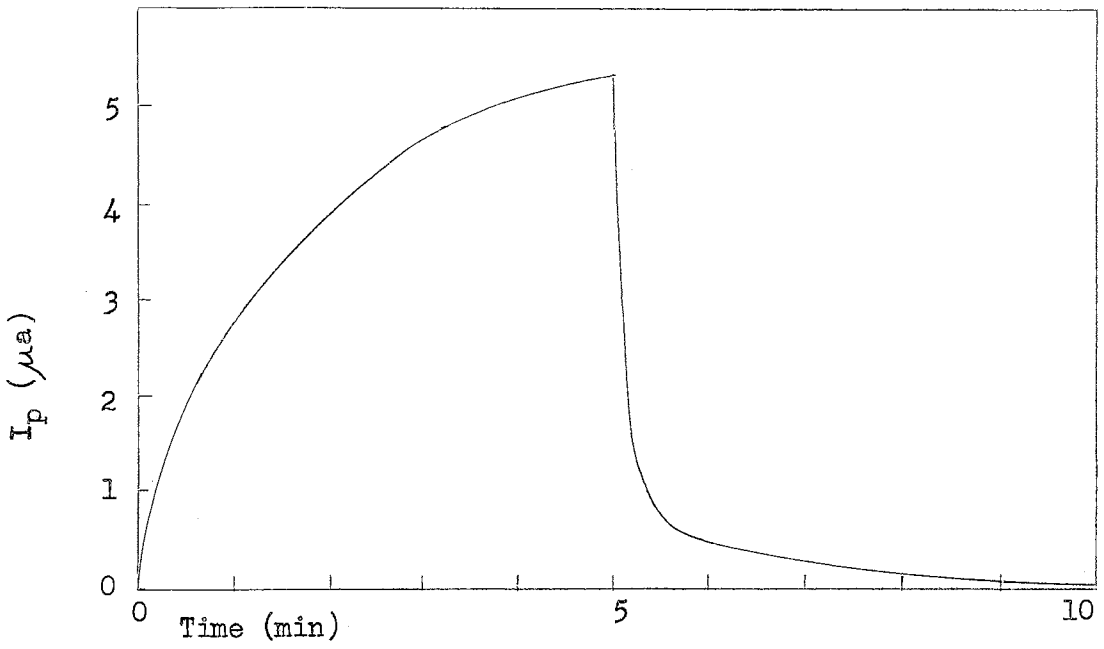

Figure 6.

Photocurrent vs. Time for Short Exposure (Sample II).

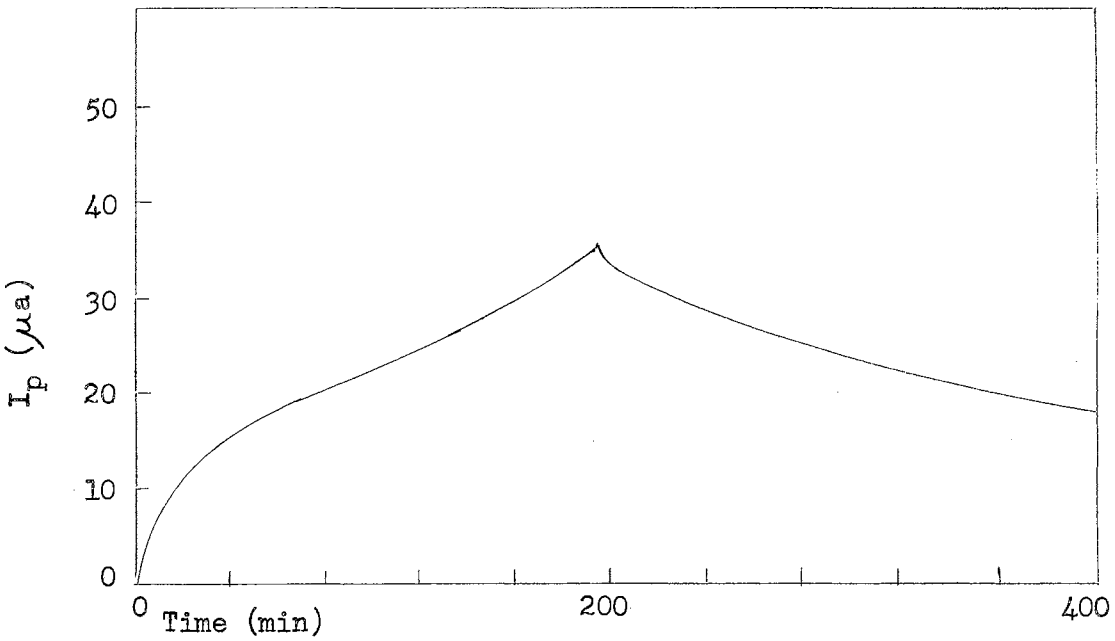

Figure 7.

Photocurrent vs. Time For Long Exposure (Sample II).

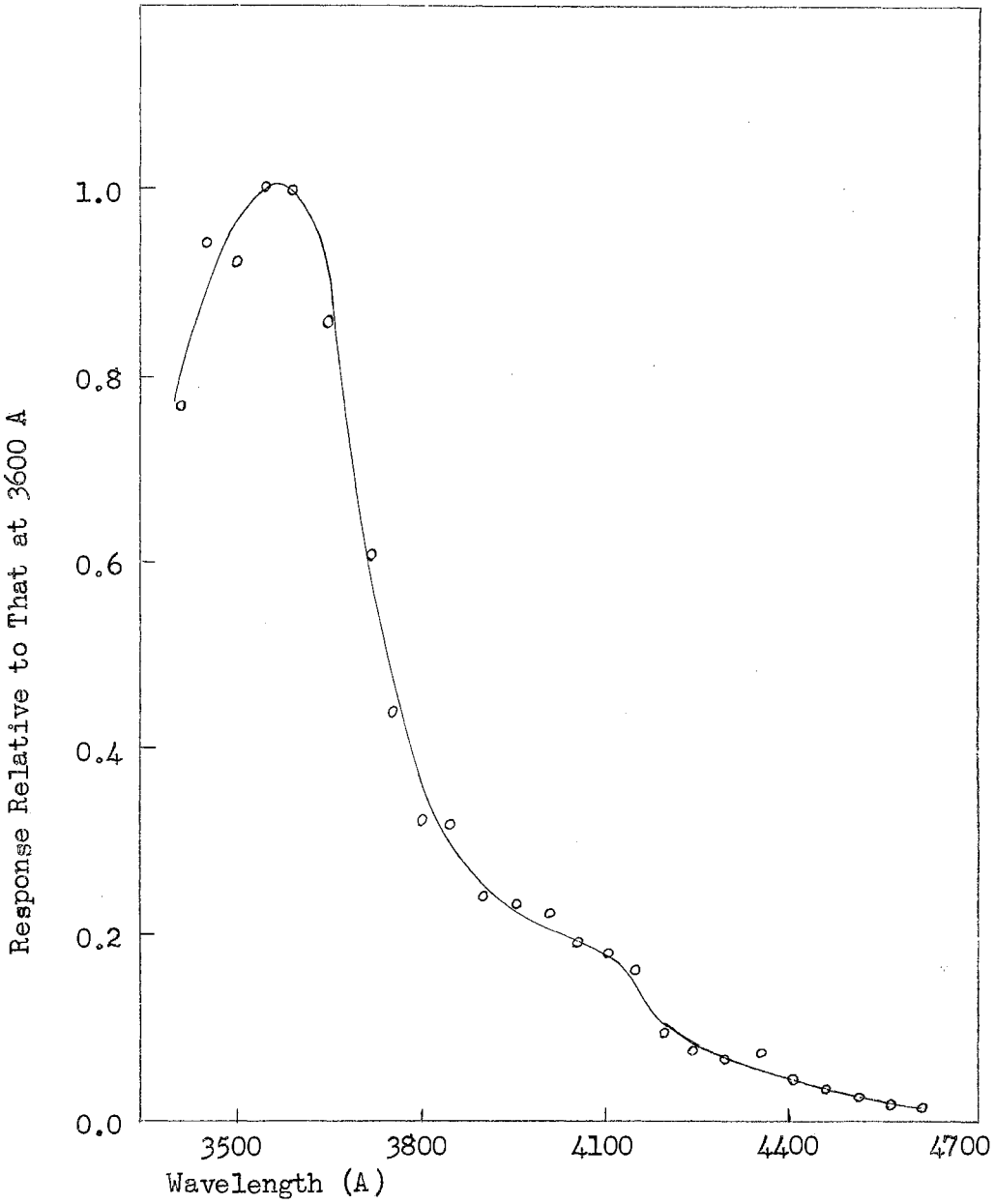

Figure 8.

Spectral Distribution of Photoconductivity for Sample II.

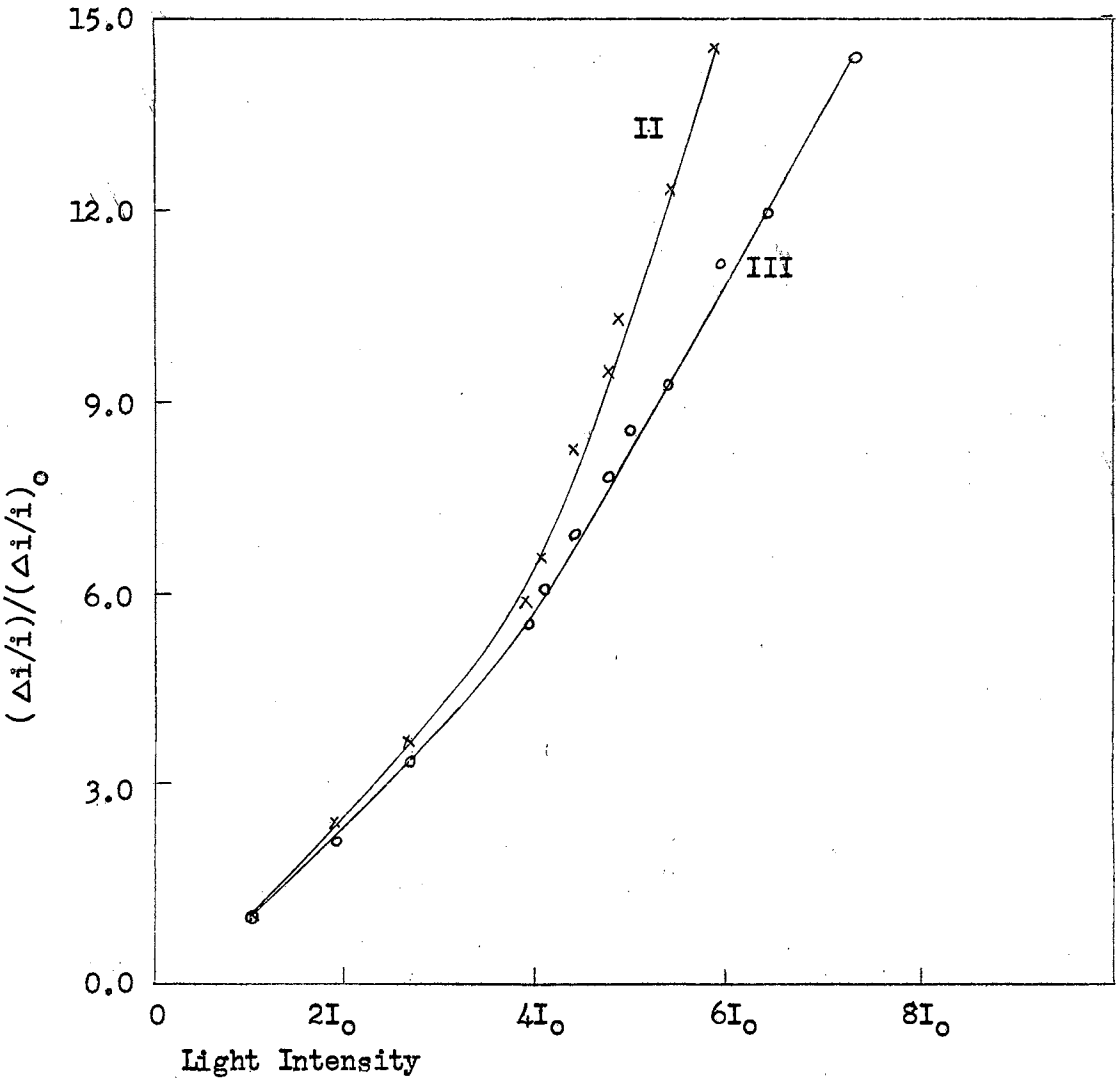

Figure 9.

Reduced Response vs. Light Intensity for Samples II and III.

$I_o = 44.9\,\mu w/cm^2$

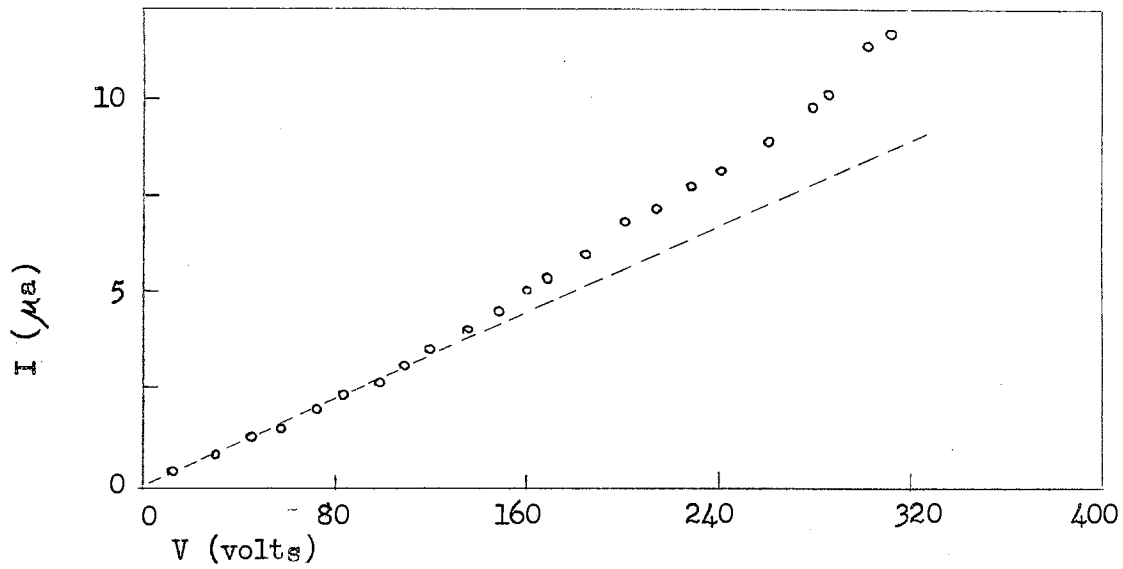

Figure 10.

Current vs. Applied Voltage for Sample III.
(Graphite Contacts)

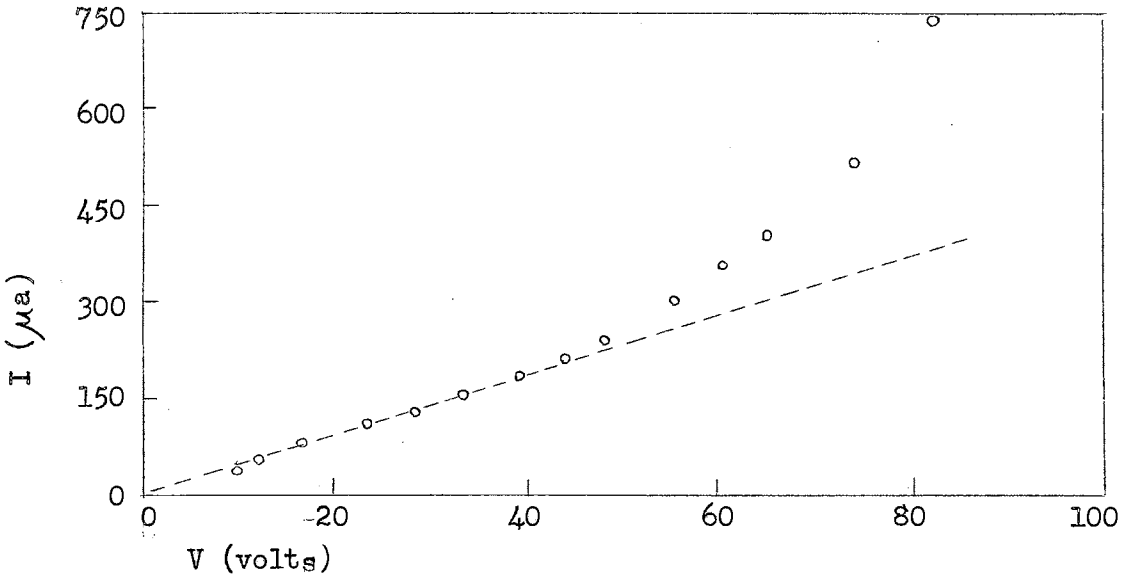

Figure 11.

Current vs. Applied Voltage for Sample III.
(Graphite Contacts)

CHAPTER VIII

SUMMARY AND CONCLUSIONS

Brief Summary of the Work

Natural stannic oxide crystals were investigated for their photoconductive behavior, with emphasis on the variation of response with the wavelength and intensity of the incident light. Variations of response with temperature and with the pressure of the ambient atmosphere received a less intensive examination. Because of the exploratory nature of the work, a number of other areas worthy of more detailed study in the future were uncovered. Among the more interesting of these were the nature of the effects at contact surfaces, the explanation of the lengthening of decay times with increasing length of exposure to light, and the importance of the part played by shallow traps in these phenomena.

Conclusions

The greatest spectral sensitivity for one-minute exposures to light was found between 3550 and 3600 A, the wavelength at which the ultraviolet absorption edge occurs. In this respect, stannic oxide crystals are found to be similar to the rutile form of titanium dioxide (2), which is of the same crystal structure. Another similarity in the photoconductive behaviors of these two oxides is the existence of a small but definite response at wavelengths considerably longer than

that of the short wavelength absorption edge. This longer wavelength response is probably a bulk effect, while the photoconductivity observed in the region of peak response is largely related to photon absorption taking place in layers near the surface. These similarities in the wavelength characteristics of the photoconductive behaviors of stannic oxide and titanium dioxide suggest that the two are basically similar in the gross features of their energy band structures.

The response vs. intensity curves obtained for the two crystals examined in detail consistently showed superlinearity at room temperature. The similarity of the characteristic curves obtained for these two samples implies that such behavior is a basic property of stannic oxide in the form used in this work. If the theory of Rose (45) is assumed to hold true in this case, the existence of at least two different classes of bound states is indicated for stannic oxide at room temperature.

A comparison of the results obtained at room temperature, dry ice temperature, and liquid nitrogen temperature indicates that as the separation between the demarcation levels is increased by lowering temperature, the percentage of recombination centers among the bound states is increased. The amount of data used in establishing this trend is small, and further investigation along these lines is in order.

The lengthening of the decay time with increasing time of exposure indicates that the density of shallow trapping centers is increased by the action of light on stannic oxide. This same conclusion can be reached by consideration of the changes observed in the rate of increase of photocurrent during an extended exposure to light of

sufficient intensity. These effects are reversible, as a crystal will regain its original electrical properties after several hours in darkness. A tenative explanation of this behavior would involve light-induced surface changes, and/or contact effects.

AC measurements indicate that carrier lifetimes shorter than 10^{-3} seconds can be found in stannic oxide, decay times of this order of magnitude and less having been observed by oscilloscope for short-period exposures ranging down to 0.002 seconds. The wide variation of decay times and sensitivities observed for stannic oxide under different conditions of temperature, ambient atmosphere pressure, and incident light energy indicate a complicated energy band structure.

Suggestions for Further Study

It has been ascertained that the energy band structure of natural stannic oxide is not simple, and much has yet to be found regarding the nature, distribution, and relative importance of the various bound states contributing to the behavior of this material. Several phases of the photoconductive behavior indicate a need for an investigation of surface effects. Plans have already been made for a study of the photoconductivity as influenced by the pressure and composition of the ambient atmosphere - with emphasis on the effects of oxygen - which should be helpful in the determination of some of the contributing processes.

The effects of partial oxidation and reduction of stannic oxide crystals should be studied, and a correlation sought between the information thus gained and that obtained from an ambient atmosphere study. A further investigation of the effects of contact materials

containing oxidizing or reducing agents should also be carried out.

Another line of investigation that would be in order is the determination of carrier mobilities and densities by the Hall method. Hall measurements over a wide range of temperatures and light intensities could be used to obtain information regarding the relative importance of holes and electrons in the photoconductive behavior and possibly to help define the types and locations of bound states in certain regions of the energy gap.

To determine the locations of shallow trapping states and obtain some indication of the relative importance of each of these, thermally stimulated current measurements should be carried out at temperatures ranging down to that of liquid nitrogen, and lower if practical.

Of great aid to all studies of the semiconducting properties of stannic oxide would be the development of a method of growing large single crystals. This would enable more accurate determinations of the effects of impurity ions and of the properties inherent in this rutile-structure oxide.

BIBLIOGRAPHY

1. Cronemeyer, D. C., and M. A. Gilleo. "The Optical Absorption and Photoconductivity of Rutile." Phys. Rev. 82, 975-976 (1951).

2. Cronemeyer, D. C. "Electrical and Optical Properties of Rutile Single Crystals." Phys. Rev. 87, 876-886 (1952).

3. Breckenridge, R. G. and W. R. Hosler. "Electrical Properties of TiO_2 Semiconductors." Phys. Rev. 91, 793-802 (1953).

4. Northrip, J. W. II. Master's Thesis, Oklahoma State University, 1958 (Unpublished).

5. Palache, C., H. Berman, and C. Frondel. "Cassiterite." Dana's System of Mineralogy. New York: John Wiley and Sons, Inc., 1944, pp. 574-581.

6. Weiser, H. B. The Hydrous Oxides. New York: McGraw-Hill Book Co., 1935, pp. 202-224.

7. Coffeen, W. W. "Ceramic and Dielectric Properties of the Stannates." J. Am. Ceram. Soc. 36, 207-214 (1953).

8. Quirk, J., and C. G. Harman. "Properties of Tin Oxide-base Ceramic Body." J. Am. Ceram. Soc. 37, 24-26 (1954).

9. Berkman, S., J. C. Morrell, and G. Egloff. Catalysis. New York: Reinhold Publishing Corp., 1940.

10. U. S. Pat. 2,617,745 (Nov. 11, 1952). Pittsburgh Plate Glass Co.

11. Dutch Pat. 73,114 (Aug. 15, 1953) N. V. Philips Gloeilampenfabriken.

12. U. S. Pat. 2,583,732 (Jan. 29, 1952) E. A. Ericsson and A. O. Jorgenson.

13. German Pat. 807,416 (June 28, 1951) E. Durrwachter.

14. Tonneson, T. H. "The Distribution of Transistor Action." Proc. Phys. Soc. (London) 65B, 737-739 (1951).

15. Verwey, E. J. W. "Oxidic Semiconductors." Semiconducting Materials Ed. H. K. Henisch. London: Butterworths Scientific Publications, Ltd., 1951, pp. 151-161.

16. Gray, T. J. "On the Properties of Semiconducting Oxides." Semiconducting Materials Ed. H. K. Henisch. London: Butterworths Scientific Publications, Ltd., 1951, pp. 180-187.

17. Gray. T. J. "Semiconductivity and Magnetochemistry of the Solid State." Chemistry of the Solid State Ed. W. E. Garner. London: Butterworths Scientific Publications, Ltd., 1955, pp. 133-142.

18. De Vore, R. J. "Refractive Indices of Rutile and Sphalerite." J. Opt. Soc. Am. 41, 416-419 (1951).

19. Gotman, J. D. "Some Anomalies in the Properties of Cassiterite." Compt. Rend. Acad. Sci. URSS 23, 470-472 (1939).

20. Himmel, H. "Optical Measurements on Cassiterite." Neues Jahrb. Mineral. Geol., Beil Bd. A64, 67-70 (1931).

21. Fischer, A. "Thin Semiconducting Layers on Glass." Z. Naturforschung 9a, 508-511 (1954).

22. Ishiguro, K., T. Sasaki, T. Arai, and I. Imai. "Optical and Electrical Properties of Tin Oxide Films." J. Phys. Soc. Japan. 13, 296-304 (1958).

23. Berton, A. "Comparison of Visible and Ultraviolet Color of Mineral Oxides and Their Hydroxides and Hydrates." Compt. Rend. 207, 625-627 (1938).

24. Ecklebe, F. "Optical Studies on Cassiterite in the Temperature Region 16-1100°C." Neues Jahrb. Mineral. Geol., Beil Bd. 66A, 47-88 (1933).

25. Thurnauer, H. "Review of Ceramic Materials for h-f Insulation." J. Am. Ceram. Soc. 20, 368-372 (1937).

26. Berberich, L. J., and M. E. Bell. "Dielectric Properties of the Rutile Form of TiO_2." J. Applied Physics. 11, 681-692 (1940).

27. Connell, L. F., and R. L. Seale. "Electrical Properties of Rutile Single Crystals." Phys. Rev. 85, 745 (1952).

28. Schusterius, C. "The Temperature Variation of the Dielectric Properties of Titanium and Tin Oxides." Z. Tech. Physik. 16, 640-642 (1935).

29. Aitchison, R. E. "Transparent Semiconducting Oxide Films." Australian J. Appl. Sci. 5, 10-17 (1954).

30. Bragg, W. L., and J. A. Darbyshire. "The Structure of Thin Films of Certain Metallic Oxides." Trans. Faraday Soc. 28, 522-529 (1932).

31. Foex, M. "Study of the Electrical Conductivity of the Oxides of Ti, Sn, and Ce as a Function of Temperature and of the Medium." Bull. Soc. Chem. France, 11, 6-17 (1944).

32. LeBlanc, M., and H. Sachse. "The Electron Conductivity of Solid Oxides with Different Valencies." Physik Z. 32, 887-889 (1931).

33. Guillery, P. "Electrical and Optical Behavior of Semiconductors. VI. Conductivity Measurements on Powders." Ann. Physik, 14, 216-220 (1932).

34. Bauer, G. "Electrical and Optical Behavior of Semiconductors. XIII. Measurements on Oxides of Cd, Tl, and Sn." Ann. Physik, 30, 433-445 (1937).

35. Zerfoss, S., R. G. Stokes, and C. H. Moore. "The Properties of Synthetic Single Rutile Crystals." J. Chem. Phys. 16, 1166 (1948).

36. Johnson, G. H. "Influence of Impurities on Electrical Conductivity of Rutile." J. Am. Ceram. Soc. 36, 97-101 (1953).

37. Johnson, G., and W. A. Weyl. "Influence of Minor Additions on Color and Electrical Properties of Rutile." J. Am. Ceram. Soc. 32, 398- 401 (1949).

38. Alexander, A. E. "Synthesis of Rutile and Emerald." J. Chem. Ed. 26, 254-257 (1949).

39. Liebisch, T. "The Layer Structure and Electrical Properties of Cassiterite." Sitzb. Kgl. Preuss. Akad. Wiss. 1911, 414-422 (1911).

40. Arzruni, A. "Kunstlicher Kassiterit." Z. fur Krystallographie XXV, 467-470 (1895).

41. Deville, H. St. C. "De la reproduction de l'etain oxyde et de rutile." Compt. Rend. 53, 161 (1861).

42. Levy, M., and L. Bourgeois. "Sur le Dimorphisme de l'acide Stannique." Compt. Rend. 94, 1365-1366 (1882).

43. Wunder, G. "Uber den Isotrimorphismus des Zinnoxyds und der Titansaure und uber die Krystallformen der Zirconerde." J. Prakt. Chem., Ser. 2, Vol. 2, 206-212 (1870).

44. Shockley. W. Electrons and Holes in Semiconductors. New York: D. Van Nostrand Co., Inc., 1950, pp. 237-246.

45. Rose, A. "Performance of Photoconductors." Proceedings of the Photoconductivity Conference Held at Atlantic City Nov. 4-6, 1954. Ed. R. G. Breckenridge, New York: John Wiley and Sons, Inc., 1956, pp. 3-49.

46. Wright, D. A. "Photoconductivity." British J. Appl. Phys. 9, 205-214 (1958).

47. Andrievskii, A. T., and V. A. Zhuravlev. "Relaxation of Photoconductivity in Stannic Oxide." Dokl. Akad. Nauk. SSSR 108, 1, 43-46 (1956).

48. Kennedy, D. R., M. Ritchie, and J. MacKenzie. "The Photosorption of Oxygen and Nitric Oxide on Titanium Dioxide." Proc. Faraday Soc. 54, 119-129 (1958).

49. Medved, D. B. "Photodesorption in Zinc Oxide Semiconductor." J. Chem. Phys. 28, 870-873 (1958).

50. Collins, R. J., and D. G. Thomas. "Photoconduction and Surface Effects With Zinc Oxide Crystals." Phys. Rev. 112, 388-395 (1958).

51. Peria, W. T. Optical Absorption and Photoconductivity in Magnesium Oxide Crystals." Phys. Rev. 112, 423-433 (1958).

52. Mitchell, E. J. W. "Impurity Scattering in Oxide Semiconductors." Proc. Phys. Soc. (London) 65B, 154-161 (1951).

VITA

James Edward Hurt

Candidate for the Degree of

Master of Science

Thesis: PHOTOCONDUCTIVITY IN STANNIC OXIDE CRYSTALS

Major Field: Physics

Biographical:

Personal Data: Born at Newton, Kansas, February 11, 1935, the son of W. Earnest and Pauline B. Hurt.

Education: Attended grade school in Kiowa and Labette, Kansas, and in Coweta, Atoka, and McAlester, Oklahoma; graduated from McAlester High School in 1953. Attended Southeastern State College, Durant, Oklahoma, from 1953 until 1955; received the Bachelor of Science degree from the Oklahoma State University, with a major in Physics, in May, 1957.